J Polym Res (2008) 15:59–65
DOI 10.1007/s10965-007-9141-7

Mechanical properties of low-density polyethylene/nano-magnesium hydroxide composites prepared by an in situ bubble stretching method

Xiu-ting Zheng · Da-ming Wu · Qing-yun Meng · Ke-jian Wang · Ying Liu · Li Wan · Dong-yun Ren

Received: 12 May 2006 / Accepted: 6 August 2007 / Published online: 12 September 2007

Abstract Low-density polyethylene/nano-magnesium hydroxide (LDPE/nano-$Mg(OH)_2$) composites have been prepared by an in situ bubble stretching (ISBS) method and simple shear method. By means of field emission scanning electron microscopy (FE-SEM) and transmission electron microscopy (TEM), it was confirmed that the ISBS method leads to a high degree of dispersion of the $Mg(OH)_2$ nanoparticles in the LDPE matrix. Furthermore, no significant re-aggregation of the nanoparticles was observed after removing the bubbles by means of high-speed grinding. The tensile strengths of nanocomposites prepared by means of the ISBS method were higher than those of materials with the same $Mg(OH)_2$ loading produced by direct blending/extrusion. The tensile strength of the nanocomposites produced by the ISBS method reached a maximum value at an $Mg(OH)_2$ content of 15 phr. In contrast, the tensile strength of composites prepared by direct blending/extrusion shows a monotonic decrease with increasing $Mg(OH)_2$ content. The improvement in mechanical properties of nanocomposites associated with the use of the ISBS method can be attributed to a more homogeneous dispersion of smaller nanoparticles.

Keywords In situ bubble stretching (ISBS) · Low-density polyethylene (LDPE) · Nano-magnesium hydroxide (nano-$Mg(OH)_2$) · Nanocomposite · Nanoparticles dispersion

X.-t. Zheng · D.-m. Wu (✉) · Q.-y. Meng · K.-j. Wang · Y. Liu · L. Wan · D.-y. Ren
Beijing University of Chemical Technology,
Beijing 100029, People's Republic of China
e-mail: wudaming@vip.163.com

Introduction

Polymer matrix nanocomposites have attracted considerable academic and industrial interest because nanoscale effects have the potential to afford significant improvements in properties such as impact resistance [1], modulus [2], thermal stability and fire resistance [3–6] compared with those of pure polymers. Nanoparticles possess rather high surface/volume ratios and surface energies however. This results in a tendency to agglomeration, especially at the temperatures and pressures typically employed in polymer processing and blending. The resulting agglomerates have dimensions of hundreds of nanometers or even micrometers, which dramatically reduces the beneficial effects associated with addition of nanoparticles. The key to exploiting the advantageous features of nanoparticles is therefore to ensure that dispersion at the nanoscale is retained in the composites.

Low-density polyethylene (LDPE) is one of the most widely used commodity plastics. Formation of nanocomposites can enhance the properties of LDPE and widen its range of applications. For instance, $Mg(OH)_2$ has been used as an effective flame retardant in LDPE [7]. However addition of such flame retardants often has an adverse effect on the mechanical properties of the polymer [8, 9], which has been attributed to the poor compatibility between additive and polymer. Nanoscale dispersion of the additive in polymers such as LDPE can ameliorate this situation [10, 11].

Both physical and chemical approaches have been explored in an attempt to solve the dispersion problem. Melt blending using conventional extruders and mixers is generally not sufficient to prevent aggregation of nanogranules. Although shearing can be an effective means of nanoparticle dispersion, prolonged high-speed shearing can induce polymer degradation. Surface chemical treatment of

nanogranules can, to a certain degree, enhance dispersion and interfacial compatibility between phases; it also reduces the surface energy however so that nanoscale effect are weakened or even eliminated. In situ intercalation or exfoliation polymerization is effective only for dispersing nano-clays having a layered structure [12–16] and cannot be used to disperse nano-magnesium hydroxide. We have previously described [10] a new process for nanoparticle dispersion which we named the in situ bubble stretching (ISBS) method and the diagram of the mechanism of ISBS dispersion process is given in Fig. 1.

This process relies on the inflation and explosion of bubbles during foaming, which efficiently disperses the nanoparticles during nanocomposite formation. The particles are first compounded with the polymer melt to give a micro-homogeneous dispersion. The mixture is then foamed. During foaming, the particles act as nucleation sites for bubble formation. The forces acting on the surface of the aggregates associated with rapid inflation of the bubbles favor particle breakdown and dispersion.

According to Tadmor and Gogos' dumbbell model for particle separation in melt laminar flow [17], the forces required to detach adhered particles by shear and tension respectively are as follows,

$$F_{r\max} = 3\pi \times \mu_r \times \dot{\gamma} \times r^2 \quad (1)$$

$$F_{e\max} = 6\pi \times \mu_e \times \dot{\varepsilon} \times r^2 \quad (2)$$

where $\dot{\gamma}$ is shear rate, $\dot{\varepsilon}$ is elongation rate, μ is the viscosity of the surrounding melt, and r is granule radius. The separation force is proportional to shear rate and elongation rate respectively. In practical terms, elongation can give more effective dispersion than simple shearing. In a twin-screw extruder, the maximum obtainable shear rate is of the order 10^2–10^3 s^{-1} whilst in the case of PS/CO_2 foaming, for example, Hee and Han reported that the bubble expansion rate can reach 10^6 s^{-1} or even higher [18]. The rapid inflation of the bubbles during the ISBS process exerts strong stretching and shearing forces on the coarse granular aggregates, enhancing their dispersion in the surrounding polymer melt. Furthermore, the melt viscoelasticity induces oscillations in bubble growth of the order of megahertz [11, 18]. Such ultrasonic cavitation leading to locally high pressures, high temperatures and shockwaves causes the particle aggregates to fragment and disperse giving nanometer-sized particles [19]. Thus, the application of an additional ISBS step leads to higher dispersion of the nanoparticles in the melt than can be obtained by a single mechanical extrusion step alone.

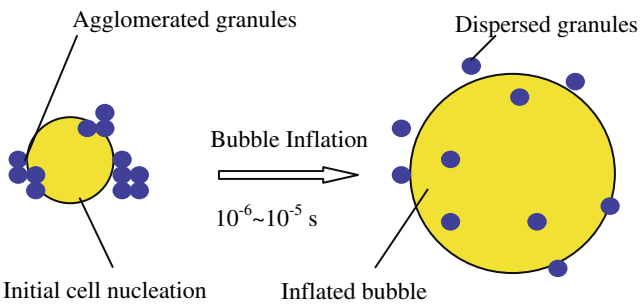

Fig. 1 Diagram of the mechanism of ISBS dispersion process

The process can be carried out in practice as follow (see Fig. 2). After blending the nanoparticles with the polymer melt in a twin-screw extruder, the mixture is further melt-foamed in a subsequent single screw extruder. The resulting composite foam is finally ground with a gas–lead grinder in order to eliminate the bubbles.

In this paper we report a study of the microstructure and tensile properties of LDPE/nano-$Mg(OH)_2$ composites prepared using the ISBS method and compare the materials with those produced by a conventional direct melt blending and extrusion process.

Experimental

Materials

Low-density polyethylene (LDPE 19E) with MFI of 2.3 g/10 min was produced by China Daqing Petrochemical. Nano-$Mg(OH)_2$ with granule size of 40–60 nm was obtained from Yixing Auxiliary Chemicals Plant. The foaming agent employed was azodicarbonamide (superfine powder, hereafter referred as AC) from Qianjiang Chuhong Chemical. Its decomposition temperature was 190–210 °C. Stearic acid was obtained from Beijing Chemical Reagent. The lubricant was paraffin oil from Changzhou Changrui Petroleum.

Preparation of LDPE/nano-$Mg(OH)_2$ nanocomposites

The nano-$Mg(OH)_2$ was first dried for 10 h at 120 °C. Mixtures of LDPE, $Mg(OH)_2$, paraffin oil and stearic acid with the required composition were first mixed in a high-speed stirrer. The compositions are listed in Table 1. These mixtures were directly extrusion pelleted using a co-rotating parallel twin-screw extruder (ZSK-25WLE, Werner & Pfleiderer, Germany) with die temperature of 190 °C and screw speed of 300 rpm.

Portions of the directly melt blended mixtures were further extrusion-foamed in a single screw extruder (PSJ-32-28A, screw diameter of 32 mm, L/D of 28, compression ratio of 3.2, Beijing Plastics Industry Unite). The weight ratio of LDPE to foaming agent (AC) was 100:0.5. Foaming was carried out at 195 °C with screw speed of

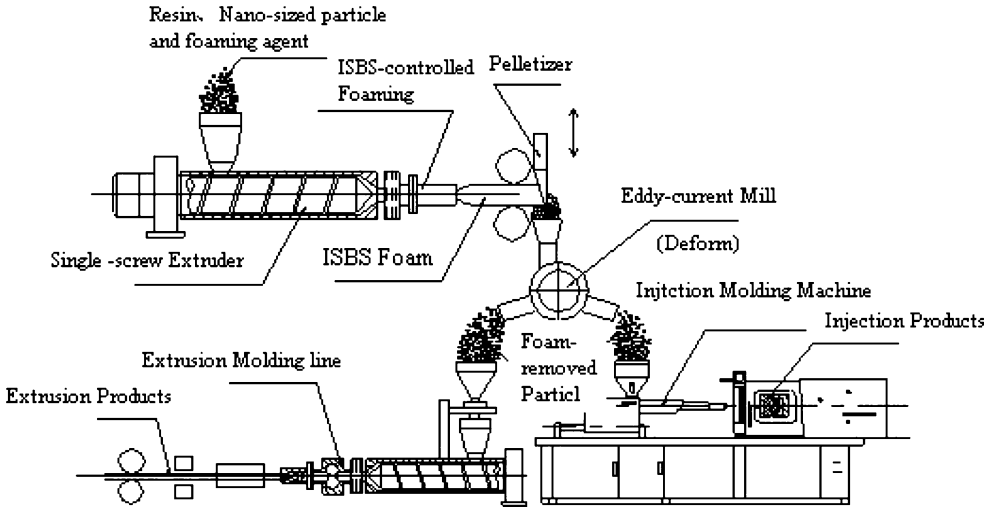

Fig. 2 Diagram of the process of nanocomposites preparation by ISBS method

100 rpm and die pressure of 10 MPa. The foamed material was then crushed using a DF180 plastics granulator and ground into a powder for subsequent defoaming under the protection of liquid nitrogen using a gas–lead grinder (Youqi, Taiwan). Finally, the powder was dried and moulded to give a standard tensile specimen using an injection molding machine (A80-210, Auckland, Hong Kong).

Morphological analysis by field emission scanning electron microscopy (FE-SEM)

The directly compounded mixtures were fractured in liquid nitrogen. The cross surface was coated with gold for observation by FE-SEM (S4700, Hitachi, Japan).

Particle size distribution

A laser particle size analyzer (MS 2000, Malvern Instruments, U.K.) was used to analyze the size distribution of dispersed particles in the sample produced by the ISBS method after defoaming with a gas–lead grinder.

Morphological analysis by transmission electron microscopy (TEM)

To investigate whether or not the dispersed nanoparticles were re-agglomerated after removal of the foam bubbles, nanocomposite samples before and after the defoaming process were observed by TEM. The prepared nanocomposites were ultra thin-sectioned using a microtome diamond knife. The cut sections of thickness 60–80 nm were collected on a 200-mesh copper grid. Micrographs were obtained using a TEM (HT-800, Hitachi, Japan) running at an accelerating voltage of 100 kV.

Mechanical properties

Tensile strength tests were conducted on an Instron-1122 universal testing instrument with a cross-head speed of 50 mm/min at room temperature according to the ASTM D638-81 standard procedure.

Results and discussion

FE-SEM of LDPE/nano-$Mg(OH)_2$ composites

Figure 3 presents the FE-SEM micrographs of the LDPE/nano-$Mg(OH)_2$ samples prepared by different methods with different contents of nano-$Mg(OH)_2$. Fig. 3a to c show the micrographs of directly extruded samples. Fig. 3d to f show the micrographs of samples further dispersed by ISBS.

Table 1 Compositions of precursor mixtures for preparation of LDPE/nano-$Mg(OH)_2$ nanocomposites

Sample no.	LDPE (phr)	Nano-$Mg(OH)_2$ (phr)	Paraffin oil (phr)	Stearic acid (phr)
0	100	0	2.5	3
1	100	10	2.5	3
2	100	15	2.5	3
3	100	20	2.5	3
4	100	25	2.5	3
5	100	30	2.5	3

phr: per hundred parts of resin

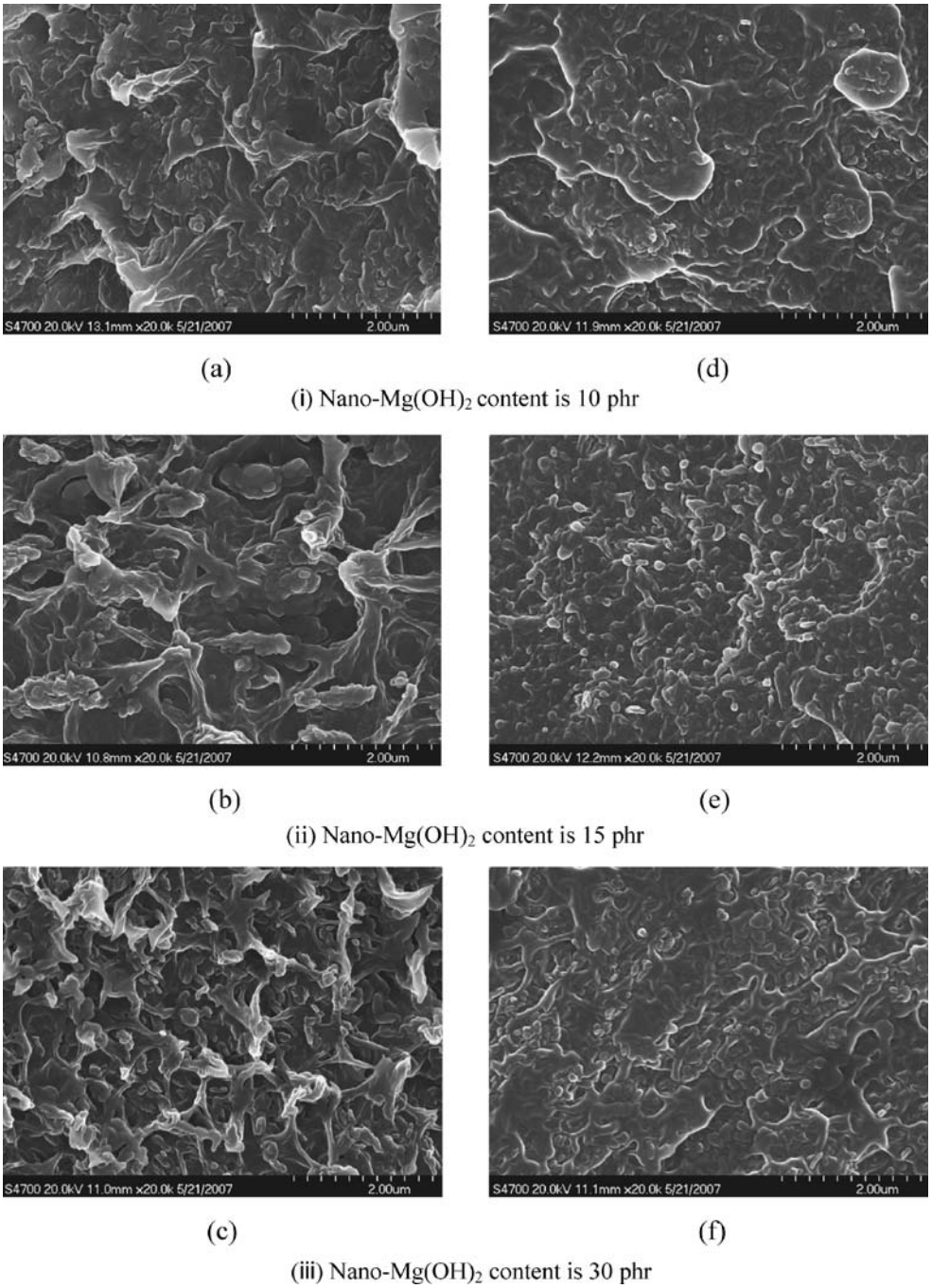

Fig. 3 FE-SEM micrographs of the LDPE/nano-$Mg(OH)_2$ sample. **a**–**c** Directly extruded and **d**–**f** further dispersed by ISBS

Fig. 3a and d show the micrographs of samples in which the content of nano-$Mg(OH)_2$ is 10 phr. And Fig. 3b and e, c and f, show the micrographs which the content of nano-$Mg(OH)_2$ is 15 and 30 phr, respectively.

Compared with Fig. 3a and d, b and e, c and f, it can be seen that with the same content of nano-$Mg(OH)_2$, the average size of the particles in the sample prepared by the twin-screw extruder is several micrometers, whereas the average size of the particles in the sample prepared by ISBS method is only several decades of nanometers and the nanoparticles are homogeneously dispersed in the polymer melt, see Fig. 3d to f. Thus it is clearly demonstrated that foaming significantly enhances the dispersion of the particles on the expanded surfaces obtained by bubble inflation during the ISBS process.

From Fig. 3d to f, it can be seen that when the content of nano-$Mg(OH)_2$ is not more than 15 phr, the dispersion is excellent. When the content increases to 15 phr, it seems to

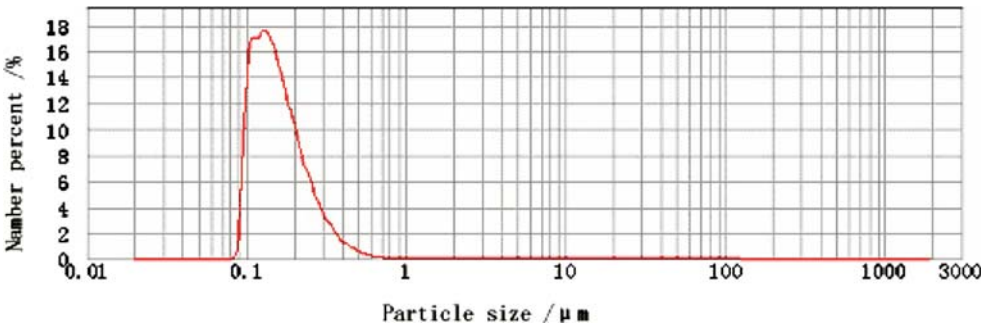

Fig. 4 Particle size distribution of LDPE/ nano-$Mg(OH)_2$ composite after grinding of the composite in order to remove the foam bubbles

get a critical value, after that the dispersion becomes poor with further increase of the content.

TEM of the composites before and after defoaming

The presence of bubbles formed during the ISBS process may adversely affect the properties of the resulting composite. Therefore, the foam composites were subsequently ground in order to eliminate the bubbles. Figure 4 shows the particle size distribution of the LDPE/nano-$Mg(OH)_2$ composite after bubble removal. The size of the particles of composite of LDPE/nano-$Mg(OH)_2$ remains well below 1 μm, suggesting that complete elimination of the foam cells has not resulted in re-agglomeration.

This is confirmed by the TEM micrograph of the defoamed nanocomposite shown in Fig. 5 which clearly shows that the $Mg(OH)_2$ particles are of nanometer scale and homogeneously dispersed in the polymer matrix. Comparison with the FE-TEM micrograph shown in Fig. 3e suggests that there is no significant increase in particle size after defoaming.

The fact that no significant re-aggregation is observed can be explained as follows. After the ISBS step, the composite was cooled from the processing temperature to room temperature. Since the strong interfacial adhesion between the $Mg(OH)_2$ particles and the resin overcomes both the resin shrinkage and the interaction between segregated particles, the embedded rigid particles in the resin do not readily re-aggregate. Furthermore, the particles

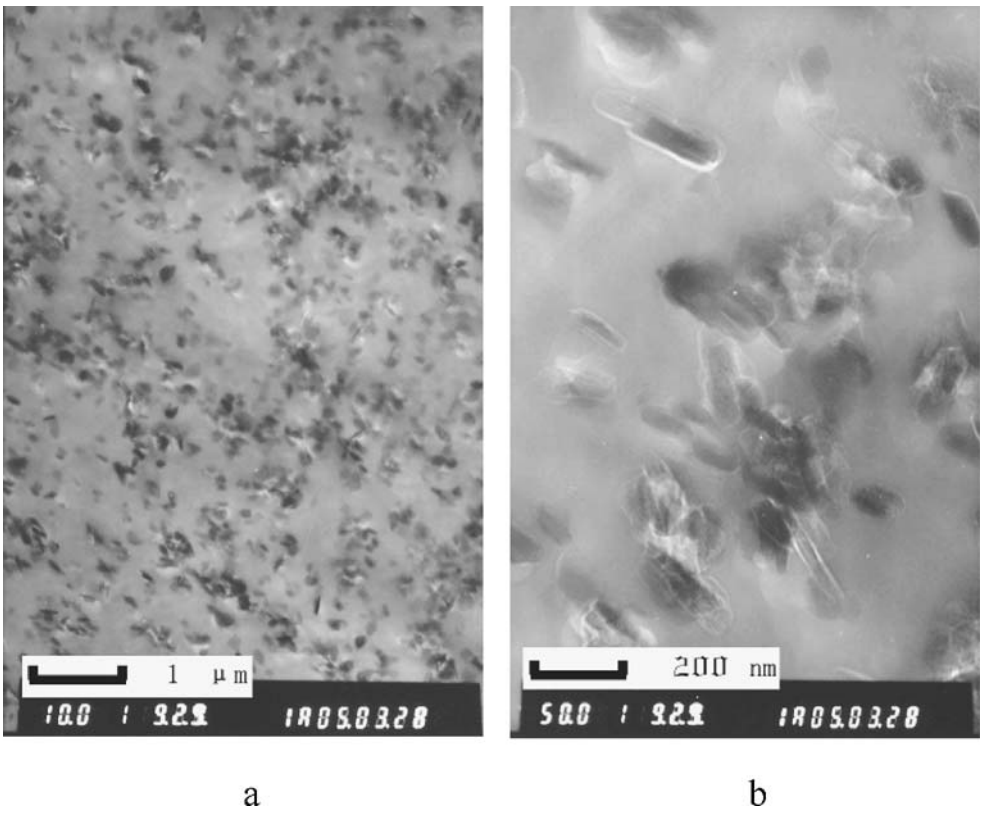

Fig. 5 TEM micrographs of the defoamed nanocomposites at **a** low and **b** high magnification (LDPE/nano-$Mg(OH)_2$=100:15)

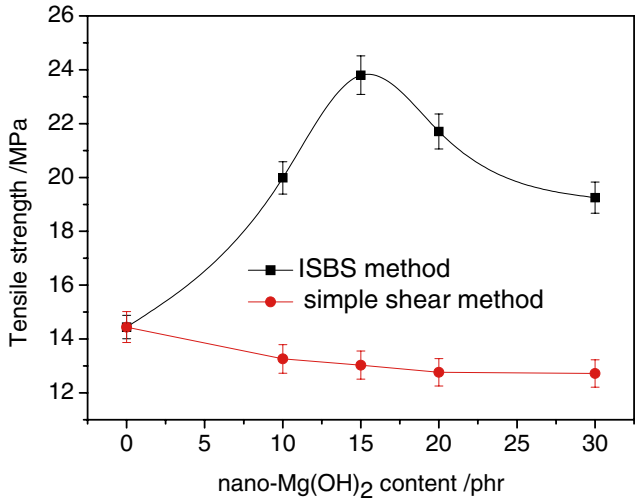

Fig. 6 Comparison of the variation in **a** tensile strength and **b** elongation at break with the content of nano-$Mg(OH)_2$ for composites produced by simple shear method and after ISBS

are compressed by the polymer during cooling because the polymer shrinks to a great extent whilst contraction of the rigid nanoparticles can be neglected. Re-agglomeration of the nanoparticles is therefore very effectively suppressed by the matrix. A similar interpretation has been proposed by Leclair and Favis [20].

Mechanical properties of LDPE/nano-Mg(OH)2 nanocomposites

The variation in tensile strength and elongation at break as a function of the loading of nano-$Mg(OH)_2$ in composites by simple shear method, i.e. by directly melt blending/extrusion and ones by ISBS are shown in Fig. 6a and b, respectively.

The tensile strength of LDPE/nano-$Mg(OH)_2$ nanocomposites obtained by the ISBS method increases with increasing nano-$Mg(OH)_2$ content up to 15 phr and then decreases at higher loadings as shown in Fig. 6a. In contrast, the tensile strengths of composites obtained by direct blending/extrusion decrease monotonically with increasing content of nano-$Mg(OH)_2$. The maximum increase in tensile strength observed after carrying out the ISBS step is approximately 80%. From Fig. 6b, it can be seen that the elongation at break of both types of composite decreases with increasing nano-$Mg(OH)_2$ content. However, the values of elongation at break for nanocomposites prepared using the ISBS step are higher than those of the conventional composites for each loading of nano-$Mg(OH)_2$.

When the content of the nano-$Mg(OH)_2$ in LDPE/nano-$Mg(OH)_2$ nanocomposites obtained by the ISBS method with a loading of not more than 15 phr, the nano-$Mg(OH)_2$ can get a dispersion by its original granules. In this case the mechanical properties of the composite improve with the increasing of the content of the nano-$Mg(OH)_2$. However, when the content of $Mg(OH)_2$ exceeds 15 phr, some aggregation of $Mg(OH)_2$ particles occurs. These re-aggregates are the weakest points in the composite which lead to earlier tensile break.

Conclusions

The ISBS process has been shown to be a very effective means of preparing LDPE/nano-$Mg(OH)_2$ nanocomposites. Subsequent grinding leads to defoaming but does not cause the dispersed nanoparticles to re-aggregate. The tensile strength and elongation at break of nanocomposites prepared by the ISBS method are superior to those prepared by direct melt blending/extrusion. The maximum tensile strength is observed for an nano-$Mg(OH)_2$ content of 15 phr. The enhanced mechanical properties associated with the ISBS method result from the effective nanoscale dispersion of the filler.

Acknowledgements This study was funded by a Key Scientific Research Project of the Chinese Ministry of Education (No. 104025) and the National Natural Science Foundation of China (No. 50673006).

References

1. Rong M, Zhang M, Zheng Y et al (2001) Improvement of tensile properties of nano-SiO_2/PP composites in relation to percolation mechanism. Polymer 42(7):3301–3304
2. Agag T, Koga T, Takeichi T (2001) Studies on thermal and mechanical properties of polyimide-clay nanocomposites. Polymer 42(8):3399–3408

3. Shelley JS, Mather PT, De Vries KL (2001) Reinforcement and environmental degradation of nylon-6/clay nanocomposites. Polymer 42(13):5849–5858
4. Fu X, Qutubuddin S (2000) Synthesis of polystyrene-clay nanocomposites. Mater Lett 42:12–15
5. Shu Z, Chen G, Qi Z (2000) Polymer/clay nano-composite and its unique flame retardance. Plastics Industry 28(3):24–26
6. Uhl FM, Wilkie CA (2002) Polystyrene/graphite nanocomposites: effect on thermal stability. Polym Degrad Stab 76(1):111–122
7. Hornsby RP, Watson CL (1989) Mechanism of smoke suppression and fire retardancy in polymer containing magnesium hydroxide filler. Plast Rubber Process Appl (11):45–49
8. Chiu SH, Wang WK (1998) The dynamic flammability and toxicity of magnesium hydroxide filled intumescent fire retardant polypropylene. J Appl Polym Sci 67(6):989–995
9. Sain M, Park SH, Suhara F et al (2004) Flame retardant and mechanical properties of natural fiber-PP composites containing magnesium hydroxide. Polym Degrad Stab 83(2):363–367
10. Wu D, Meng Q, Liu Y et al (2003) In situ bubble-stretching dispersion mechanism for additives in polymers. J Polym Sci 41: 1051–1058
11. Meng Q, Wu D (2004) A study of bubble inflation in polymers and its applications. Phys Lett A 327:61–66
12. Medellin-Rodriguez FJ, Burger C, Hsiao BS et al (2001) Time-resolved shear behavior of end-tethered nylon 6-clay nanocomposites followed by non-isothermal crystallization. Polymer 42(21):9015–9023
13. Yeh JM, Lion SJ, Lin CY et al (2002) Anticorrosively enhanced PMMA clay nanocomposite materials with quaternary alkylphosphonium salt as an intercalating agent. Chem Mater 14(1):154–161
14. Kawasumi M, Okada A (1997) Preparation and mechanical properties of polypropylene clay hybrids. Macromolecules 30(20): 6333–6338
15. Zhang L, Wang Y, Wang Y et al (1998) Preparation and property of clay/SBR rubber nanocomposites. Special Purpose Rubber Products 19(2):6–9
16. Ma J, Qi Z, Zhang S (2001) Synthesis and characterization of elastomeric polyurethane/clay nanocomposites. J Appl Polym Sci 3:325–328
17. Tadmor Z, Gogos G (1979) Principles of polymer processing. Wiley, New York
18. Hee JY, Han CD (1982) AIChE J 28(6):1002–1008
19. Li T, Yin Q (1995) Ultrasonic chemistry. Science Press, Beijing
20. Leclair A, Favis BD (1996) The role of interfacial contact in immiscible binary polymer blends and its influence on mechanical properties. Polymer 37(21):4723–4728